CIELAB based system for burn depth estimation

Aurora Sáez, Begoña Acha, Carmen Serrano; Signal Processing and Communications Department, University of Seville, Spain

Abstract

Successful cure of a burn injury depends highly on the first treatment. Burn depth is traditionally defined in three degrees. Estimation of depth degree is carried out by visual evaluation of the wound by the specialized dermatological experts. This type of evaluation includes a high degree of subjectivity. In the literature it can found objective methods for determining the depth of the burn by processing of digital photographic images. However, these methods estimate only one degree per burn wound despite the fact that it is common to find all three types within the same burn wound. In this paper a classification system to estimate the different depth degrees that a burn wound can present, is proposed. A color characterization algorithm is initially applied to the photographic images. A color and texture features extraction based on the $L^*a^*b^*$ color space and the chromatic opponent channels is carried out. The classifier used is a Fuzzy-ARTMAP neural network. This neural network performs a pixel-based classification to estimate the different depth degrees present in burn wound image. The system has been tested with 60 images. A success rate of around 80% has been achieved.

Introduction

The burn is depicted as a traumatic lesion provoked by several possible agents (thermal, chemical, mechanical, or electrical) involving different skin layers to a certain degree. Assessment of the clinical situation is based on evaluation of the total body surface of the burns, and estimation of burn depth [1]. Visual assessment of the wound is crucial [2]. In the majority of cases, the surgical indication for excision depends upon the visual evaluation of the wound by the specialized dermatological experts. Burn depth is traditionally defined in three degrees [1]. The first degree correspond to a shallow wound. The aspect is red. Only the superficial layer of the epidermis is involved. Superficial second degree burns usually present as blister, once the blister is removed uniform redness can be observed. Deep second degree burns also present blisters, but after removal, the aspect is white or similar to patchwork. Third degree burns involving the subdermal structures. Lesions present with a white color and brown. Primary wound burn strategy depends on burn wound assessment.

The first treatment to a burned patient strongly depends on the total burned surface area and the depth of the burns present in it. This first treatment is enormously correlated to the favorable evolution of the patient [3]. As the cost of maintaining a burn treatment unit is high, it would be desirable to have an objective or automatic system to give a first assessment at primary health-care centers, where there is a lack of specialists [4, 5]. The World Health Organization demands that, at least, there must be one bed in a Burn Unit for each 500,000 inhabitants. So, normally, one Burn Unit covers a large geographic area. If a burn patient appears in a medical centre without a Burn Unit, telephone communication is usually established between the closest hospital with a Burn Unit and the local medical centre, where the non-expert doctor describes subjectively the colour, size and other aspects considered important for burn characterization. The result in many cases is the application of an incorrect first treatment, or unnecessary transportation of the patient, involving high Healthcare cost and psychological trauma for patients and family.

In the related bibliography, it can found that there is a tendency to investigate objective methods for determining the depth of the burn in order to reduce the subjectivity and the high experience requirement that visual inspection demands. In this sense, there are works trying to evaluate burn depth by using thermographic images [6, 7], terahertz pulsed imaging [8], polarization-sensitive optical coherence tomography [9] and laser Doppler imaging [10]. The main disadvantage of these methods is the complexity and cost of the image acquisition system.

In [11] a clinically feasible system for automatic burn wound classification based on the use of a digital photographic camera was designed, in which, the following clinical needs were met: the system cost was low, the system was easy to use by a physician or nurse and the system preserved the essential characteristics of the burn wounds required for diagnosis (color and texture). In this system, the image was acquired following a standardized protocol and processed to get the information required for assessing the burn depth. Image-processing algorithms to isolate the burn from the rest of the scene (segmentation), and to give the depth of the segmented burn part (classification) were designed. The system estimated automatically only one grade per burn image, however, unfortunately, burn depth assessment is rarely that simple. This is because few burns are of a uniform depth. Indeed, it is universally recognised that the depth of most burns tends to be mixed [13] [14] [15]. The deepest injury is usually at the center of a burned area. In this paper a burn depth estimation for each pixel in the image is proposed. In addition, the use of the uniform color space $L^*a^*b^*$ instead of $L^*u^*v^*$, used in [11], is proposed, and a different preprocessing of the burn image for color characterization has been applied.

The rest of the paper is organized as follows: Section 2 summarize the background, disadvantages and proposed improvements. The methodology is introduced in Section 3. The experimental results are explained in Section 4 and some conclusions are presented in Section 5.

Background

In 2005 [11] a system based on digital color photographs, which performed a burn color image segmentation and classification was proposed. For this purpose the authors designed a colorimetric characterization algorithm, a segmentation algorithm and classification method to estimate burn depth. However, this system has mainly three weaknesses, which are explained below.

- Colorimetric characterization algorithm. This algorithm [12] was motived by the fact that manufacturers normally do not publish either the red (R), green (G), blue (B) primaries of the camera or the color temperature of the flash. The authors needed to determine a transformation matrix to convert from measured RGB coordinates to device-independent color representation system. Based on the Macbeth ColorChecker DC chart, which is supplied with

data giving the CIE XYZ chromaticity coordinates of each chip under D50 illuminant, a method was proposed. The method found the transformation matrix from RGB under unknown illuminant to XYZ under D50 and corrected the non uniformity of the illumination as well as the spatial non uniformity of the camera sensitivity. However, its main disadvantage was the computational cost, due to its iterative nature.

- Usage of L*u*v*. The CIE $L^*u^*v^*$ and $L^*a^*b^*$ color spaces, abreviated CIELUV and CIELAB, respectively, were both recommended in 1976. The L^* (lightness), C^* (chroma) and h (hue) coordinates are the cylindrical representation of the same spaces. These spaces extend tristimulus colorimetry to three-dimensional spaces with dimensions that approximately correlate with the perceived lightness, chroma, and hue of a stimulus [16]. This was accomplished by incorporating features to account for chromatic adaptation and nonlinear visual responses. The main aim in the development of these spaces was to provide uniform practices for the measurement of color differences. However, since 1976, CIELAB has become almost universally used for color specification and particularly color difference measurement. At this time there appears to be no reason to use CIELUV over CIELAB [16].
- Estimation of only a depth degree per burn image. The classification method used a Fuzzy ARTMAP neural network. The input parameters were the average feature values, based on $L^*u^*v^*$, extrated from the segmented region, considered as burn. Therefore, each burn was classified in only one depth degree. However, commonly a burn patient has mixed burns [3].

Methodology

The main aim of this paper is the correct estimation of the different burn depths that can appear in an image. There are three main types of burn depths [3]:

1. *Superficial dermal burn.* The epidermis and part of the dermis are destroyed. It is characterized by the presence of blisters (usually brown color) and/or a bright red color.
2. *Deep dermal burn.* Its pink-whitish color characterizes it.
3. *Full-thickness burn.* All the skin thickness is destroyed and skin grafts are needed. It is characterized by a beige-yellow or a dark brown color.

An example of them it is shown in Figure 1. Although a burn wound is classified in three classes, it can present five different appearances.

1. Blisters: they are superficial dermal burns with a bright texture and a rose-brown color.
2. Bright red: they are superficial dermal burns with bright red colors and wet appearance.
3. Pink-white: they are deep dermal burns with a dotted appearance.
4. Yellow-beige: first appearance of full-thickness burns.
5. Brown: second appearance of full-thickness burns.

In this section, the methodology followed in this research is presented, which involves image preprocessing, features extraction, features selection and burn depth estimation.

Preprocessing

Physicians for the assessment of a burn take into account some texture aspect and mainly color [3]; therefore, an image-

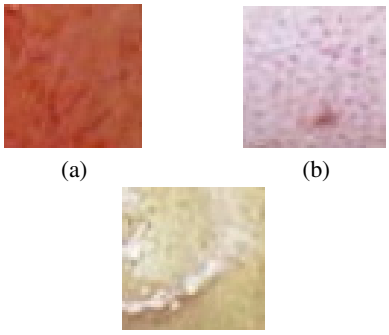

Figure 1. *Different appearances that could present a burn, (a) Superficial dermal, (b) Deep dermal,(c) Full thickness (beige).*

acquisition system must preserve this property to the highest accuracy possible. The main problem encountered in the analysis of digital photographs of burn wounds is that, in practical situations, the illumination conditions in hospitals are uncontrolled. As a result, the measured pixel values depend on varying and unknown illuminants. This problem is due to the camera cannot perform the chromatic adaptation that the human eye automatically performs. Thus, a preprocessing step to prevent burn images from having different appearances when captured under different illumination conditions is clearly required.

The proposed preprocessing algorithm transforms the RGB values captured with the camera under an unknown illuminant to sRGB values under D50. This colorimetric characterization algorithm was proposed in [17]. The method was based on the Gretag-Macbeth Color Checker target [18]. The authors used the Macbeth ColorChecker DC chart with 240 color chips. It is supplied with data giving the CIE XYZ chromaticity coordinates of each chip under D50 illuminant. The algorithm creates interpolation curves using spline cubic interpolation in a plane whose x axis is the component captured with the camera(R, G or B) under unknown illumination conditions and the y axis is the same component under D50. Interpolation is based on points obtained from the gray chips of the photographed chart under unknown illuminant and their RGB values under D50 illuminant, provided by the manufacturer. An example of these curves is shown in Fig. 2. These interpolation curves are applied to the photographed images under the same unknown illuminant that Macbeth ColorChecker DC chart was captured. The RGB values of these images under the unknown illuminant are matched with RGB values under D50 illuminant.

In order to illustrate the performance of the algorithm, a purple color sheet was photographed under four different illuminants: a halogen lamp, fluorescent lights, a xenon flash, and afternoon sunlight. Fig. 3 shows the photographs obtained under the different illuminants before and after the characterization step. It can be observed that, after the characterization procedure, the four photographs present similar colors.

Features extraction

Once the preprocessing step is applied to burns images, to isolate the burn from the rest of the scene is required. In this paper, this task is not addressed. We use images manually segmented because of the mainly aim is develop a system to estimate the burn depth. However, automated segmentation methods can be found in the literature [11].

Burn depth estimation by physicians depend strongly on color perception and on some basic texture aspects such as moist

aspect. As it have already mentioned blisters and different colors (red, pale pink, white, and tan) may be present in the burn image. Thus, in the proposed system a set of feature that characterize perceived color and texture is extracted from the segmented burn wound. These features are based on color and statistical moments derived from the histogram, which are considered sufficient to analysed texture aspects taken into account by physicians. The proposed descriptors related to color are: red component (R), green component (G), blue component (B), lightness (L*), a* component (a*), b* component (b*), chroma (C) and saturation (S). In addition, the two opponent chromatic channels, red-green (R-G) and yellow-blue (Y-B), are included. The red-green (R-G) channel is a good discriminant between red and white colors. The difference value between red band and green band for a white color is significantly lower than for a red color. The proposed descriptors related to texture are: standard deviation, skewness and kurtosis of red component (R), green component (G), blue component (B), lightness (L*), a* component (a*), b* component (b*), chroma (C) and saturation (S).

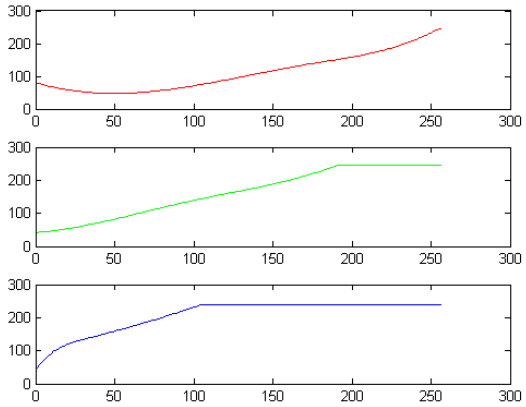

Figure 2. *Interpolation curves of R,G and B. RGB values of the photographed chart under unknown illuminant are represented in abscissas axis. RGB values of the chart under D50 illuminant are represented in ordinate axis.*

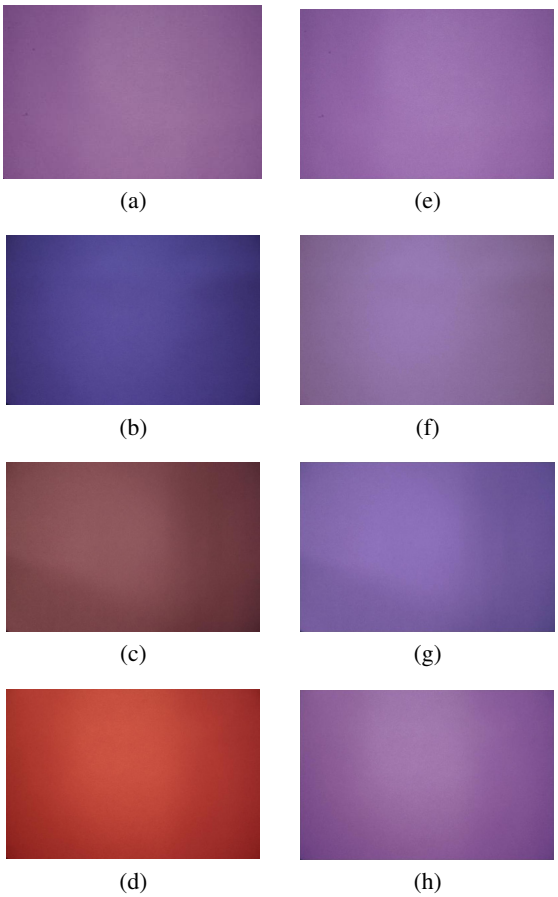

Figure 3. *A purple sheet photographed under four different illumination conditions: (a) a xenon flash, (b) afternoon sunlight, (c) fluorescent lights, and (d) a halogen lamp. (e)-(h) The characterized images corresponding to the images in (a)-(d), respectively.*

Features selection

The discrimination power of the features set was analyzed using the well known methods Sequential Forward Selection (SFS) and Sequential Backward Selection (SBS) [19]. They were implemented via the Fuzzy-ARTMAP neural network, which is detailed in the following subsection. Feature selection is performed to select the best subset from the input space.

To apply these two methods, fifty 49x49 pixel images per each appearance were used. As there are five appearances, there are 250 49x49 pixel images in all. The 250 49x49 pixel images show only one burn appearance (no healthy skin or background). Each 49x49 pixel image was validated by two physicians as belonging to a particular depth. The selection performance was evaluated by fivefold cross validation (XVAL). In this sense, the disadvantage of sensitiveness to the order of presentation of the training set, that the SBS and SFS methods present, was diminished. To perform the XVAL method the 50 images per burn appearance were split into five disjoint subsets. Four of these subsets (40 images per appearance) served as training set for the neural network, while the other one (10 images) was used as validation set. Then, the procedure was repeated interchanging the validation subset with one of the training subsets, and so on till the five subsets were used as validation sets. The final classification error was calculated as the mean of the errors for each XVAL run.

The subset of features with higher discrimination power was: a^* coordinate (a^*), B coordinate (B), standard deviation of b^* (σ_{b^*}), saturation (S), skewness of R coordinate (s_R), opponent channel red-green (R-G) and standard deviation of a^* coordinate (σ_{a^*}) **??**.

Classifier

The classifier used is a Fuzzy-ARTMAP neural network, as it has been mentioned above. This neural network architecture was developed by Grossberg and Carpernter et al [20] and is based on Adaptive Resonance Theory (ART). Fuzzy-ARTMAP is a supervised learning classification architecture for analog-value input pairs of patterns, each individual input is mapped to a class label. The advantages that Fuzzy-ARTMAP offers are the well-understood theoretical properties, an efficient implementation, clustering properties that are consistent with human perception, and a very fast convergence.

Classification Result

The proposed features set based on L*a*b* color space and RGB components was analysed using the SFS ans SBS methods described in the previous Section, with the purpose of determining the subset of features with the most discriminant power. The minimum classification error obtained was 2.1%. It was obtained

both in SFS and in SBS, however in the case of SFS method the number of selected features was smaller. This subset of features (shown in Table 1) was: a^* coordinate (a^*), B coordinate (B), standard deviation of b^* (σ_{b^*}), saturation (S), skewness of R coordinate (s_R), oppponent channel red-green (R-G) and standard deviation of a^* coordinate (σ_{a^*}).

Table I. Results of features selection

Method	Feature subset	Average error
SFS	a^*, B, σ_{b^*}, S, s_R, R-G, σ_{a^*}	2.1%

The selected features subset was used as input to the neural network. The network classified each pixel of the segmented burn instead of providing an only classification value for the complete segmented burn wound. For the calculation of the standard deviation and skewness, a neighbourhood of 10×10 pixels around of central pixel is taken into account. This yields a pixel-based classification that allow to estimate the different burn depths that can appear in an image. An example is shown in Fig. 4, where it can be observed a white area classified as deep dermal at the center of the wound and a bigger red superficial dermal area. In Fig. 5 is shown a full thickness burn in its two appearance, beige and brown. The burn injury in Fig. 6 presents a third depth degree central area surrounded by a superficial dermal burn. The color coding utilized for the system in the output image is: green to blister, red to superficial dermal, blue to deep dermal, white to full thickness (beige), brown to full thickness (brown).

The method was tested with 60 images. This images belong to diagnosed patients by physicians at the moment of the arrival to the Burn Unit. A 35% of the images were diagnosed as mixed burn (the patient presented more than one depth degree). The proposed system estimated the same depth degrees that physicians had diagnosed in a 80% of these images.

For the rest of the images, 65%, only one depth degree appeared predominantly. The table 2 summarizes the classification results for these images. The success percentage obtained for each burn depth is shown in comparison with obtained results in [11]. It is shown that the proposed method outperforms the method proposed in [11].

Table II. Classification Results

Burn depth	Success percentage in [11]	Success percentage proposed method
Superficial dermal	86.36%	86.11%
Deep dermal	83.33%	85.71%
Full thickness	77.27%	81.25%
Average	**82.26%**	**84.35%**

Conclusions

The aim of the paper is burn depth estimation in digital color photographs. In the literature, this task has been already addressed, however these works have not taken in account the fact that it is common for a patient to have burns of different depths. In this paper this fact is taken account and a pixel-based classification has been proposed to achieve it. The method involves a first step of preprocessing, in which the RGB values of the images photographed under unknown illuminants are matched with RGB values under D50 illuminant. Features based on the CIELAB uniform color space are used to estimates the depth degree of each pixel of the burn injury. The 35% of the images in the dataset used to test the system were classified in two different burn depths by the physicians. The system classified the 80% of these images into the same depth degrees that physicians diagnosed. It can be conclude, therefore, that the proposed system is able to distinguish between different burn depths present in an image.

As the rest of the images of the dataset (65%) was diagnosed in one depth degree, the classification results of these images are compared with results obtained in [11]. In the mentioned work a burn depth estimation was performed by using a Fuzzy-ARTMAP neural network with features based on CIELUV color space and each image was classified into one of the possible depth degree. The classification results presented in this paper

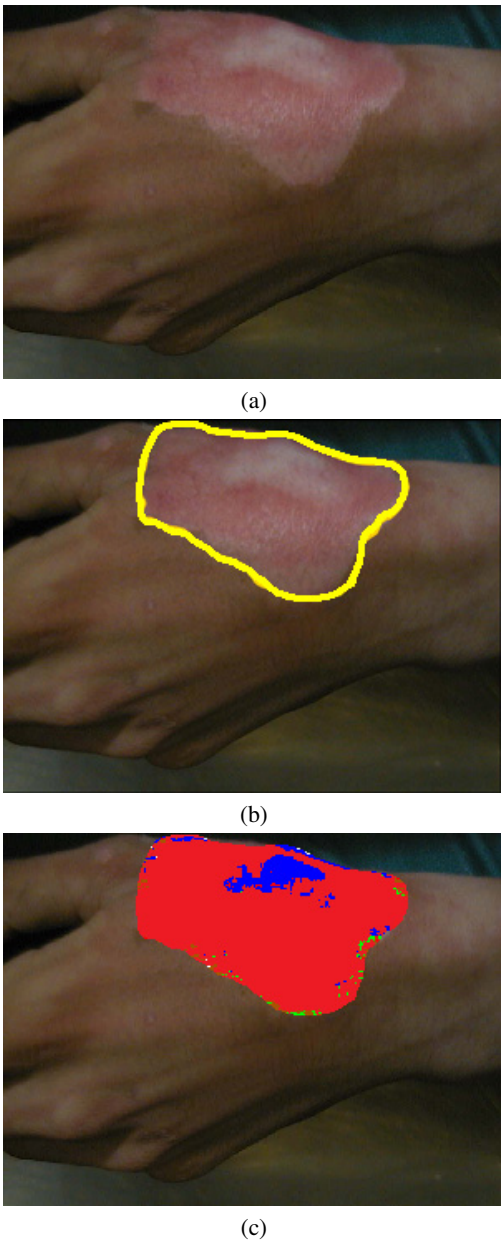

(a) (b) (c)

Figure 4. *a) Original image: deep second degree at the center of a wound with superficial second degree. b) Manually segmented burn injury. c) Burn depth estimation (green=blister, red=superficial dermal, blue=deep dermal, white=full thickness (beige), brown=full thickness (brown))*

show that the proposed method outperforms the method proposed in [11].

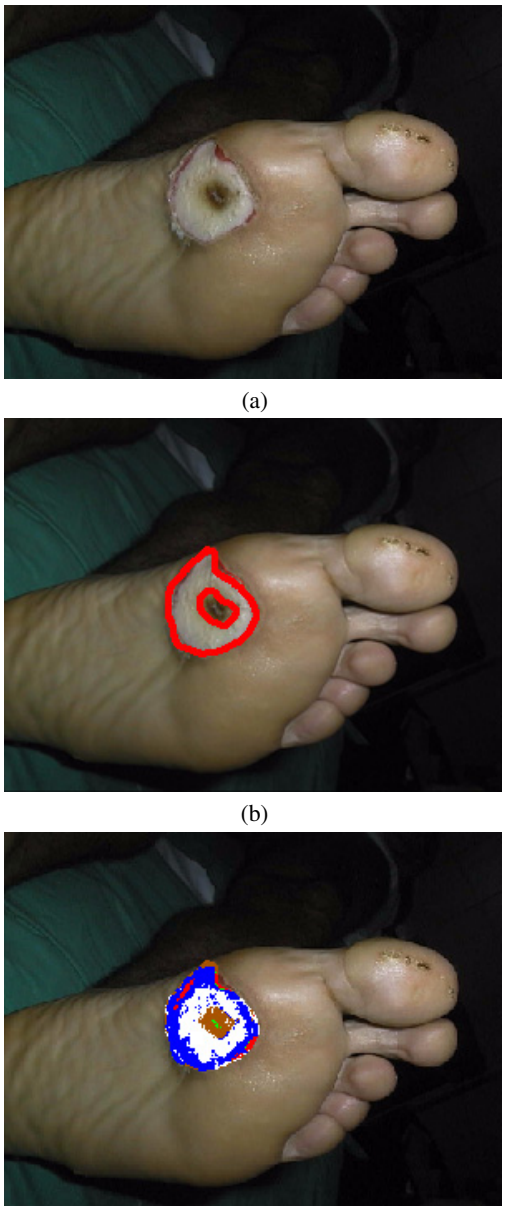

(a) (b) (c)

Figure 5. *a) Original image of third degree burn with deep second degree around it. b) Manually segmented burn injury. b) Manually segmented burn injury. c) Depth burn estimation (green=blister, red=superficial dermal, blue=deep dermal, white=full thickness (beige), brown=full thickness (brown))*

References

[1] H., Hyakusoku, D.P., Orgill, L., Teot, J.J., Pribaz, R. Ogawa (Eds.), Color Atlas of Burn Reconstructive Surgery (Springfield, 2010)

[2] Jackson DM, (1953) The diagnosis of the depth of burning. Br J Surg 40:588?596

[3] Clarke,J.A.: A Colour Atlas of Burn Injuries. Chapman & Hall Medical, London (1992)

[4] Serrano, C., Roa, L., Acha, B.: Evaluation of a telemedicine platform in a burn unit. In Proceedings of the IEEE International Conference on Information Technology Applications in Biomedicine, pp. 121?126, Washington DC, (1998)

[5] Roa, L., Gmez-Ca, T., Acha, B., Serrano, C.: Digital imaging in remote diagnosis of burns. Burns 25 (7), 617-623 (1999)

[6] Romero-Mandez, R., Jimenez-Lozano, J.N., Sen, M., Javier Gonzalez, F.: Analytical solution of the Pennes equation for burn-depth

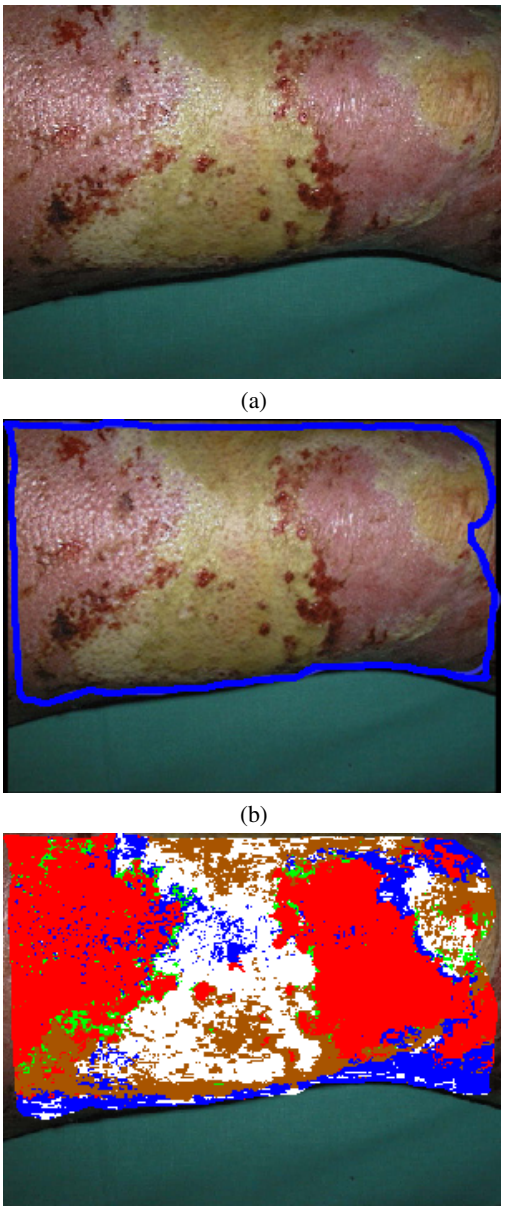

(a) (b) (c)

Figure 6. *a) Original image of third degree burn surrounded by a superficial dermal burn. b) Manually segmented burn injury. c) Depth burn estimation (green=blister, red=superficial dermal, blue=deep dermal, white=full thickness (beige), brown=full thickness (brown))*

determination from infrared thermographs. Mathematical Medicine and Biology 27 (1), 21-38 (2009)

[7] Ruminski, J., Kaczmarek, M., Renkielska, A., Nowakowski, A.: Thermal parametric imaging in the evaluation of skin burn depth. IEEE Transactions on Biomedical Engineering 54 (2), art. no. 14, 303-312 (2007)

[8] Huang, S.Y., Macpherson, E., Zhang, Y.T.: A feasibility study of burn wound depth assessment using terahertz pulsed imaging. Proceedings of the 4th IEEE-EMBS International Summer School and Symposium on Medical Devices and Biosensors, ISSS-MDBS 2007 , art. no. 4338310, 132-135 (2007)

[9] Pierce, M.C., Sheridan, R.L., Park, B.H., Cense, B., De Boer, J.F.: Burn depth determination in human skin using polarization-sensitive optical coherence tomography. Proceedings of SPIE - The International Society for Optical Engineering 4956, 263-270 (2003)

[10] Monstrey, S.M., Hoeksema, H., Baker, R.D., Jeng, J., Spence, R.S., Wilson, D., Pape, S.A.:Burn wound healing time assessed by laser Doppler imaging. Part 2: Validation of a dedicated colour code for image interpretation. Burns 37 (2), pp. 249-256 (2011)

[11] Acha, B., Serrano, C., Acha, J.I., Roa, L.M.: Segmentation and classification of burn images by color and texture information. Journal of Biomedical Optics 10 (3), 1-11, (2005).

[12] Serrano, C., Acha, B., Sangwine, SJ.: Colorimetric calibration of images of human skin captured under hospital conditions. Proceedings of the 10th Congress of the International Colour Association AIC, 1, 773-776, Granada, Spain, (2005)

[13] Hettiaratchy S, Papini R (2004) Initial management of a major burn: assessment and resuscitation. Br Med J 329: 101-3

[14] Monstrey S, Hoeksema H, Verblenen J, Pirayesh A, Blondeel P (2008) Assessment of burn depth and burn wound healing potential. Burns 34: 761-9

[15] Enoch S, Roshan A, Shah M (2009) Emergency and early management of burns and scalds. Br Med J 338: 937-9

[16] Fairchild, M.D., Color Appearance Models, (Wiley-IS&T) 2005, pg. 78-80.

[17] Sáez, A., Acha, B., Serrano, C. : Colorimetric Calibration of Images Captured Under unknown Illuminants. Proceedings of the 11th Congress of the International Colour Association (Aic), Sidney, Australia (2009)

[18] Tannenbaum, B.: Webinar Color Image Processing with MATLAB. June 28th (2007)

[19] Fukunaga, K.: Introduction to Statistical Pattern Recognition. 2nd edition, Morgan Kaufmann (Academic Press), San Diego, CA, (1990)

[20] Carpenter, G.A., Grossberg, S., Markuzon, S., Reynolds, J.H.: Fuzzy-ARTMAP: A Neural Network Architecture for Incremental Supervised Learning of Analog Multidimensional Maps. IEEE Trans. on Neural Networks, 5, 698-713(1992)